TENSILE AND FATIGUE FRACTURE OF DISCONTINUOUSLY REINFORCED ALUMINUM (DRA)

N. Chawla, J.J. Williams, G. Piotrowski, and R. Saha

Department of Chemical and Materials Engineering
Arizona State University
Tempe, AZ 85287-6006, USA

ABSTRACT

The tensile and fatigue fracture processes in discontinuously reinforced aluminum (DRA) are described in this paper. In tension DRA exhibits planar fracture of the brittle reinforcement particles and ductile microvoid growth and coalescence in the aluminum matrix. Particle strength, strength of the particle/matrix interface, and matrix strength control the tensile behavior of the material. Fatigue fracture is controlled by surface defects and rogue-inclusions, particularly if they are larger than the reinforcement particle size. At elevated temperature, creep-fatigue interactions contribute to an enhancement in damage, particularly in the form of diffusion-assisted void growth and cavity formation.

KEYWORDS

Tension, fatigue, fracture, metal matrix composite, discontinuously reinforced aluminum.

INTRODUCTION

Discontinuously reinforced aluminum (DRA) alloys provide significantly enhanced properties over conventional monolithic aluminum, such as higher strength, stiffness and fatigue resistance, while still maintaining weight savings over other structural materials [1-4]. While continuous fiber reinforcement provides the most effective strengthening (in the direction of the reinforcement), particle reinforced composites are more attractive because of their cost-effectiveness, isotropic properties, and their ability to be processed using similar technology used for monolithic materials. In this paper, we provide an overview of the fracture behavior of discontinuously reinforced aluminum, with an emphasis on the tensile and fatigue fracture behavior of particle reinforced systems.

TENSILE FRACTURE

The reinforcing phase in DRA, typically a ceramic, is much stiffer than aluminum. Thus, a significant fraction of the applied load is initially borne by the reinforcement, by load transfer from the matrix. Since the ceramic phase has a much lower strain to failure than the metal matrix, the particles will fracture prior to failure of the composite, provided that the particles have a critical aspect ratio for load transfer to take place. If the particle/matrix interface is weak,

however, interfacial debonding and particle pullout is the preferred damage mechanism. The incorporation of particles in the matrix also results in an increase in "apparent work hardening." The term "apparent" is used here because the higher observed work hardening rate is a simple function of lower matrix volume (by incorporation of the particles) and not necessarily due to a change in work hardening mechanisms. Thus, the higher work hardening rate observed in the composites is due to geometric constraints imposed on the deformation of the matrix by the presence of the reinforcement. When the matrix is significantly work hardened, the matrix is placed under a very large degree of constraint with an inability for strain relaxation to take place by deformation. This causes the onset of void nucleation and propagation, which take place at a lower far field applied strain than that observed in the unreinforced material.

Figure 1 shows the mating surfaces obtained after tensile fracture of an Al-Cu-Mg (2080)/SiC/20_p-T6[1] composite (average particle size of 23 μm). The SiC particles fracture in a planar, brittle fashion, while evidence of microvoid growth and coalescence is observed in the matrix. Notice that the particle/matrix interface remains intact, indicating that the shear strength at the interface was higher than the particle tensile strength. Due to the angular nature of the particles, mating fracture surfaces must be observed to ensure that particle fracture did indeed take place.

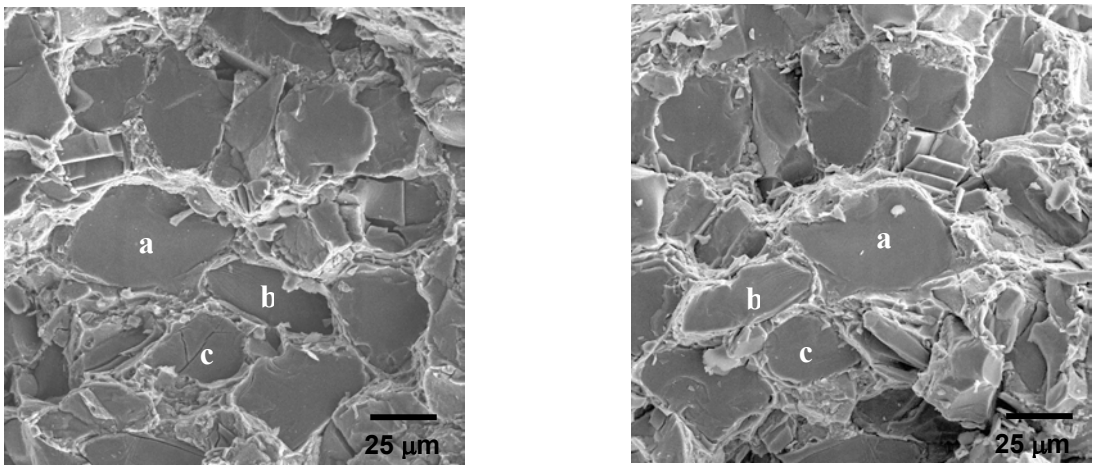

Figure 1: Tensile fracture in DRA. Planar fracture is observed in the particle, accompanied by ductile fracture in the matrix. Mirror images from mating surfaces are shown. The letters indicate examples of mating particles.

Table I shows the tensile strength and fraction of particles pulled-out, for a given particle size and matrix aging treatment. It is well known that the strength of ceramics is controlled by flaws, and that the probability of a strength-limiting flaw being present increases with material volume. Thus, the larger the particle size, the lower the particle strength, and the lower the ultimate tensile strength of the composite. It is interesting to note, however, that particle size itself does not completely control the ultimate tensile strength of the composites. This is readily apparent by the significant decrease in composite strength with severity of overaging, for a given particle size. The rate of strength decrease with overaging is almost identical for both composites. Clearly, as the matrix becomes weaker, dislocation bypass of the precipitates in the matrix

[1] We follow the standard notation for metallic composites designated by the Aluminum Association. The matrix alloy is followed by the reinforcement composition. The latter is denoted as a particulate reinforcement by the subscript 'p.' The volume fraction can also be introduced in this notation followed by the heat treatment, e.g. 2080 matrix reinforced with 20% SiC, peak-aged, would be denoted as 2080/SiC/20_p-T6.

becomes more predominant, and void nucleation and matrix tearing take place at lower applied stresses.

Table I. Effect of Particle Size and Overaging on Tensile Strength and Particle Fracture Characteristics of 2080/SiC/20_p-T8 Composites

Average Particle Size	Aging Treatment	Tensile Strength (MPa)	Fraction of Particles Pulled-out (%)
6 μm	T8-peakage	576	7.8
6 μm	peak + 24 h at 200°C	489	8.5
6 μm	peak + 24h at 225°C	410	9.5
23 μm	T8-peakage	484	5.7
23 μm	peak + 24h at 200°C	414	5.1
23 μm	peak + 24h at 225°C	348	5.6
23 μm	peak + 24h + 250°C	290	5.5

A very small fraction of particles is pulled out in both composites. Since the particle strength is lower than the interface strength, particle fracture will take place first and particle pullout will not be predominant. With an increase in particle strength (a decrease in particle size), a larger fraction of the particles will have a higher strength than the interfacial strength, so a slightly larger fraction of particles are pulled out. It is interesting to note that the extent of pullout does not change significantly with severity of overaging, indicating that, while the matrix strength is lowered significantly, that the interfacial bond strength remains relatively unchanged. It should be noted that the fraction of fractured particles decreases significantly with an increase in distance from the fracture surface [5]. This can be attributed to the large local plastic strain on the fracture plane [6]. A slight overestimation of the extent of particle fracture may take place since the crack takes a path of least resistance resulting in a non-planar fracture surface. Recent results from polished cross-sections taken from the center of the gage section of the tensile specimens, however, indicate that while the extent of particle fracture is significantly reduced immediately below and with increasing distance from the fracture plane, the trends are consistent with those shown in Table I [5].

FATIGUE FRACTURE

Ambient temperature fatigue fracture

Fatigue fracture in monolithic alloys is typically controlled by defects or inclusions, often at the surface of the material [7]. This phenomenon is also quite prevalent in DRA [8-11]. Processing-related defects in the form of exogeneous inclusions (frequently Fe-rich) or particle clusters play a significant role in controlling fatigue strength, particularly when the inclusion is much larger than the SiC particle size. The rogue inclusions act as stress concentrators that increase the local stress intensity in the material and promote easy crack nucleation. Crack initiation during fatigue takes place at these defects, which are typically located at the surface of the specimen, Fig. 2. This is because inclusions at the surface are more highly stressed than inclusions completely within the matrix, so a higher stress concentration and, thus, higher probability for crack initiation is present

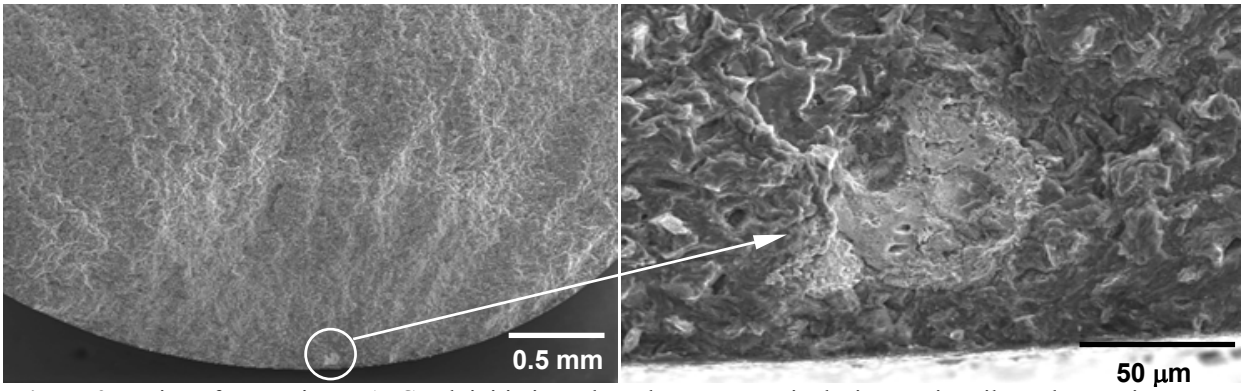

Figure 2: Fatigue fracture in DRA. Crack initiation takes place at rogue inclusions, primarily at the specimen surface.

at the surface. A given inclusion in the composite, however, will be subjected to a lower stress than in the unreinforced alloy, due to "load sharing" by the reinforcement particles. In extruded materials, the overall size of inclusions is also lower in composites since the ceramic reinforcement particles break the brittle inclusions into smaller sizes during extrusion.

Fatigue fracture of DRA exhibits two distinct fracture morphologies, Fig. 3. In the propagation region (region 1 in Figure 3) striations are often observed. After stable crack propagation, a fast fracture region is typically observed (region 2 in Figure 3). Because of the high crack velocity associated with this portion of the fracture surface, large-scale particle fracture takes place. The propensity for striation formation is controlled by the particle size, and thus, the interparticle spacing. As the interparticle spacing decreases, the degree of constraint due to triaxality of stress increases, so striation formation is hindered and the dominant damage mechanism changes to void formation [12]. Striation orientation and spacing in DRA seem to depend on individual matrix grain orientation with respect to the loading axis, Fig. 4. Figure 4 also shows the larger striation spacing in the low cycle fatigue regime, as compared to a specimen fractured in the high cycle fatigue regime. As the magnitude of stress increases, the step-like crack growth will be of a larger amplitude.

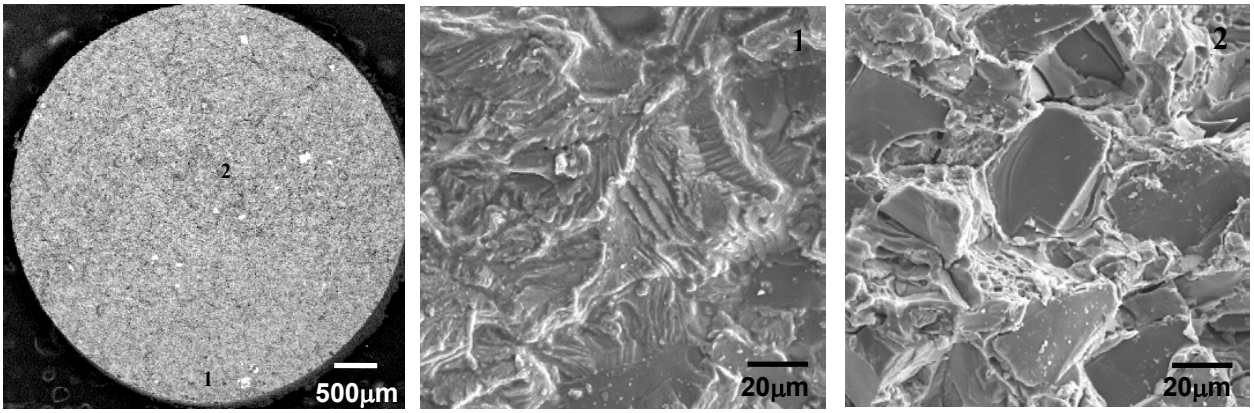

Figure 3: Fatigue morphology in DRA. Striations are observed in the stable crack propagation region (marked 1), while particle fracture is predominant in the fast fracture region (marked 2).

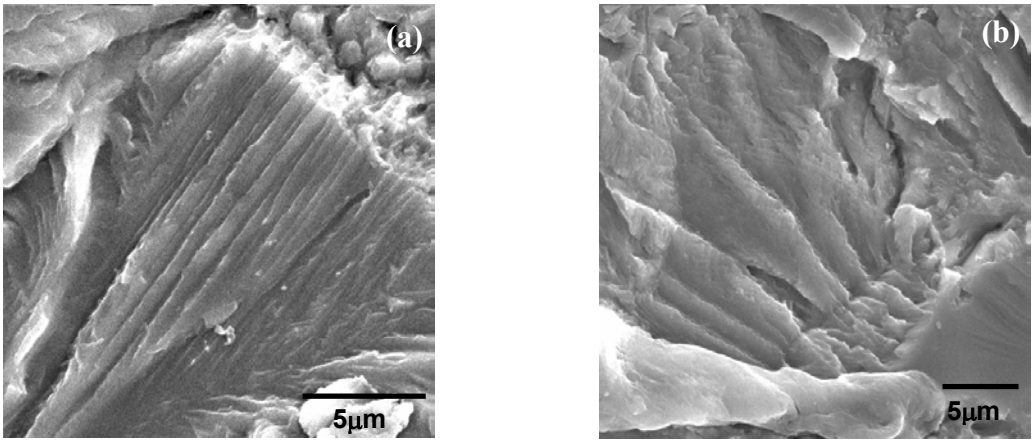

Figure 4: Fatigue striations in the matrix of DRA: (a) Finer striation spacing in high cycle fatigue and (b) larger spacing in low cycle fatigue.

It is interesting to note that in the low cycle regime, cracks seem to originate relatively early in fatigue life (around 10% of total life). In the high cycle regime, on the other hand, crack initiation can occur quite late (after about 70-90% of the life of the specimen). Figure 5 shows data on two different composites systems [9,10]. The transition from crack propagation becomes dominant in the low cycle regime, compared to most of the fatigue life being spent initiating a crack in the high cycle fatigue regime. While crack growth is relatively unimpeded in unreinforced materials, Fig. 6(a), crack growth is hindered by mechanisms such as crack deflection and crack trapping in the composite, Fig. 6(b). Crack propagation is more significant in the low cycle fatigue regime, since a much greater fraction of the life is spent in propagating the crack.

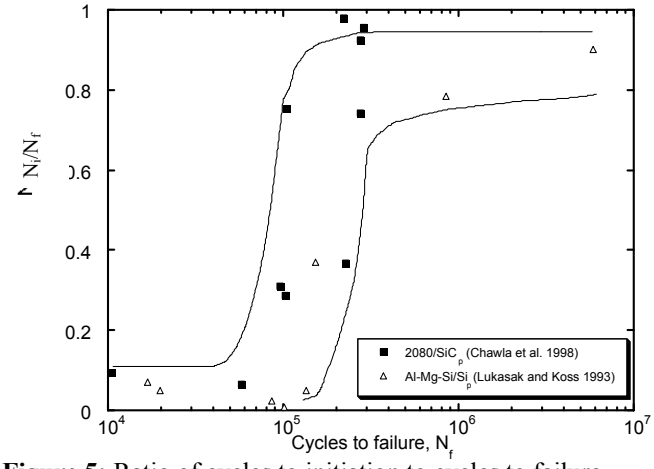

Figure 5: Ratio of cycles to initiation to cycles to failure (N_i/N_f) versus fatigue life for two different composites systems. Notice the transition from crack propagation being dominant in the low cycle regime, compared to most of the fatigue life being spent initiating a crack in the high cycle fatigue regime.

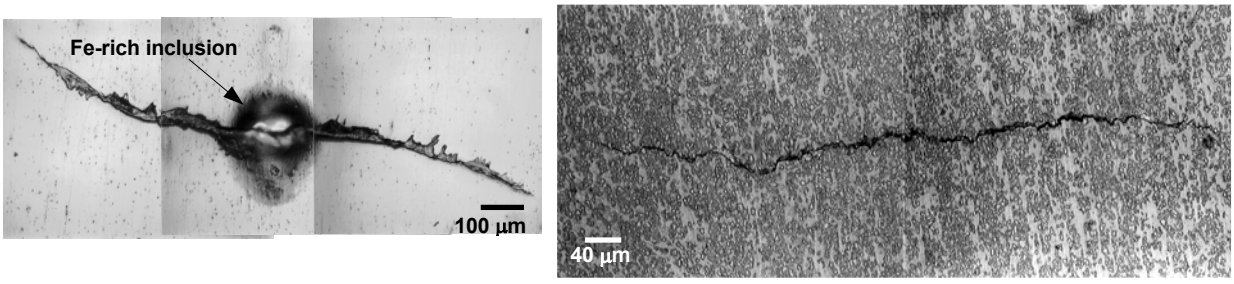

Figure 6: Fatigue crack initiation and growth in (a) unreinforced 2080 Al and (b) in 2080/SiC$_p$ composite. Notice that crack growth is hindered by mechanisms such as crack deflection and crack trapping in the composite.

Elevated temperature fatigue fracture

At elevated temperature, diffusion-assisted processes combine with fatigue processes. Interfacial decohesion and void growth at the particle/matrix interface and particle corners, as well as in the matrix of the composite take place, Fig. 7. It appears that microvoid nucleation and coalescence in

the matrix also seem to have taken place prior at fracture. During the fatigue process, void growth also takes place at angular corners of the particles, the particle/matrix interface, and in the matrix, Fig. 7. It may be reasonable to speculate that cavity growth at elevated temperatures is further enhanced by cyclic loading via diffusion and cyclic slip mechanisms. It should be noted that at elevated temperatures (150-170^{o}C) the decrease in fatigue strength is more significant than the decrease in the yield strength. Thus, some of the proposed mechanisms described above, e.g., diffusion-assisted void growth at elevated temperature, may be responsible for the higher decrease in fatigue strength versus yield strength.

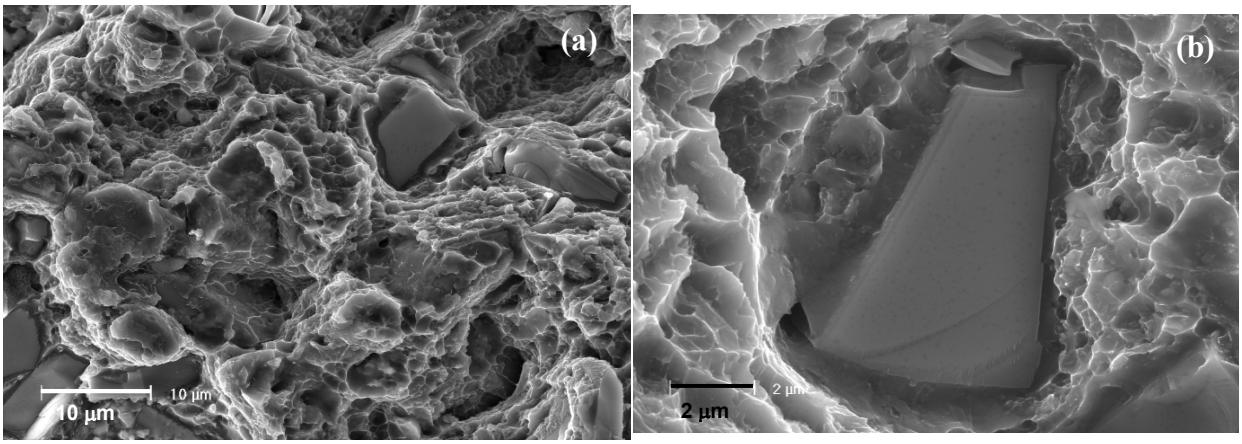

Figure 7: Elevated temperature fatigue fracture in DRA: (a) Diffusion assisted void growth in the matrix and (b) evidence of void growth at stress concentrations, such as sharp particle corners.

REFERENCES

1. Chawla, K.K. (1997). *Composite Materials - Science and Engineering*. 2nd edition, Springer-Verlag, New York.
2. Clyne, T.W. and Withers, P.J. (1993). *An Introduction to Metal Matrix Composites*. Cambridge University Press, Cambridge.
3. Lewandwoski, J.J. (2000). In: *Comprehensive Composite Materials*, pp. 151-187, Kelly, A. and Zweben, C. (Eds.). Elsevier Press, Oxford.
4. Chawla, N. and Allison, J.E. (2001). In: *Encyclopedia of Materials: Science and Engineering*, (2001), in press, Ilschner, B. and Lukas, P., (Eds.). Elsevier Press, Oxford.
5. Williams, J.J., Piotrowski, G., Saha, R., and Chawla, N., (2001) unpublished work.
6. Singh, P.M., and Lewandowski, J.J., (1993) *Metall. Trans*. 24A, 2531.
7. Suresh, S. (1998). *Fatigue of Materials*, p. 132. Cambridge University Press, Cambridge.
8. Chawla, N. and Shen, Y.L. (2001) *Adv. Mater. Eng*. 3, 00.
9. Chawla, N., Andres, C., Jones, J.W., and Allison, J.E. (1998) *Metall. Mater. Trans*. 29A, 2843.
10. Lukasak, D.A. and Koss, D.A. (1993) *Composites* 24, 262.
11. Chawla, N., Jones, J.W., and Allison, J.E., (1999). In: *Fatigue '99*, Wu, X.R. and Wang, Z.G. (Eds.). EMAS/HEP.
12. Sugimura, Y. and Suresh, S. (1992) *Metall. Trans.* 23A, 2231.

ACKNOWLEDGMENTS

The authors acknowledge the support of United States Automotive Materials Partnership (USAMP) and the Department of Energy through contract ACJ-6423. We are also grateful to Dr. Warren Hunt Jr. for supplying some of the materials used in this study.